Measurement of the ^{87}Rb-^{129}Xe spin-exchange cross section

C. H. Volk, T. M. Kwon, and J. G. Mark
Litton Guidance and Control Systems, 5500 Canoga Avenue, Woodland Hills, California 91364
(Received 9 October 1979)

The ^{87}Rb-^{129}Xe spin-exchange cross section has been measured in N_2 buffered cells as a function of the N_2 density using an alkali vapor magnetometer technique. The strong dependence of the spin-exchange cross section on the N_2 density indicates a significant role for the Rb-Xe van der Waals molecule in the spin-exchange process. Our data have allowed us to estimate the Rb-Xe molecular formation rate, which is in reasonable agreement with previous measurements. The extrapolated binary spin-exchange cross-section term is found to be $\sigma_{ex}\bar{V}^2 = 1.5\times10^{-10}$ cm^{4}sec^{-2}.

I. INTRODUCTION

The transfer of angular momentum from an electronically polarized alkali atom to an unpolarized noble-gas nucleus in spin-exchange collisions has been the subject of both experimental and theoretical investigations. Bouchiat, Carver, and Varnum[1] first observed the nuclear polarization of ^{3}He used as the buffer gas for the optical pumping of natural Rb vapor. The spin-exchange process was studied in more detail by Gamblim and Carver[2] and then subsequently by Fitzsimmons, Tankersley, and Walters,[3] who did a preliminary study of the effects of aluminosilicate containers on the attainable nuclear polarization. More recently Sobell[4] considered spin-exchange effects of Na with He, H_2, and D_2 in the relaxation of optically polarized Na vapor. Experimental determinations of the alkali-atom-noble-gas nuclear spin-exchange cross section have been in good agreement with Herman's calculations,[5] in which he attributed the spin exchange to the contact hyperfine interaction between the noble-gas nucleus and the alkali valence electron.

We report here our study of the spin-exchange process between optically oriented Rb vapor and the noble-gas nucleus ^{129}Xe, which has nuclear spin, $I=\frac{1}{2}$. Some preliminary aspects of this work were previously published.[6] We observe in our work the transverse relaxation of ^{129}Xe after it has been polarized in collisions with the oriented Rb vapor. Measurements of the relaxation rate are done as a function of both the cell temperature and the buffer gas density. From the measurements of the relaxation rate as a function of temperature, one can deduce the spin-exchange cross section knowing the Rb density. The buffer gas density dependence of the cross section yields information concerning the role of the Rb-Xe van der Waals molecules in the alkali electronic noble-gas nuclear spin-exchange process.

II. THEORY

Herman[5] has shown that the spin-exchange mechanism between an alkali valence electron and a noble-gas nucleus can be described in terms of a contact hyperfine interaction governed by the effective Hamiltonian

$$H_{eff} = \hbar\gamma\vec{I}\cdot\vec{S}, \tag{1}$$

where $\hbar$ is Plank's constant divided by 2π, γ is the strength of the interaction, $\vec{I}$ is the spin angular momentum of the noble-gas nucleus, and $\vec{S}$ is the electronic spin of the alkali atom.

If we neglect the nuclear spin of the alkali atom, then the spin exchange between the alkali atom and the ^{129}Xe noble-gas nucleus reduces simply to that of spin exchange between two spin-$\frac{1}{2}$ systems. Designate the expectation value of the longitudinal component of nuclear polarization of the noble-gas atom as $\langle I_L\rangle$ and the expectation value of the longitudinal component of the electronic polarization of the alkali atom as $\langle S_L\rangle$, then it can be shown that the time rate of change of the nuclear polarization due to spin exchange is given by[7-10]

$$\langle\dot{I}_L\rangle = -T_{ex}^{-1}(\langle I_L\rangle - \langle S_L\rangle), \tag{2}$$

where T_{ex}^{-1} is the spin-exchange rate between the noble-gas nucleus and the alkali atom, which is given in terms of the interaction strength

$$T_{ex}^{-1} = T_f^{-1}\tfrac{1}{2}\frac{\langle\gamma\rangle^2\tau_c^2}{1+\langle\gamma\rangle^2\tau_c^2}, \tag{3}$$

where T_f^{-1} is the collision frequency, $\langle\gamma\rangle$ is an average interaction strength, and τ_c is the correlation time of the interaction. The spin-exchange rate can also be written in terms of a spin-exchange cross section

$$T_{ex}^{-1} = N_A\sigma_{ex}\bar{V}, \tag{4}$$

where N_A is the alkali number density, σ_{ex} is the spin-exchange cross section, and $\bar{V}$ is the alkali-

atom-noble-gas-atom relative velocity. An expression for the spin-exchange cross section was derived by Herman[5]:

$$\sigma_{ex}=\frac{2}{3}\,\frac{8\pi g_n\mu_N\mu_B u_1(b_0)^2\eta(b_0)^2 b_0}{3\hbar\bar{V}}\,I(I+1)\sigma_{kin}\,, \tag{5}$$

where g_n is the nuclear gyromagnetic ratio of the noble-gas atom, μ_N is the nuclear magneton, μ_B is the Bohr magneton, $u_1(b_0)^2$ is the probability density for locating the alkali valence electron at a distance equal to the internuclear separation from the alkali nucleus, $\eta(b_0)$ is the exchange enhancement factor, b_0 is the kinetic radius for the collision pair, the $\sigma_{kin}=\pi b_0^2$ is the kinetic cross section.

The transverse nuclear polarization is found to obey a similar equation:

$$\langle\dot{I}^+\rangle=T_{ex}^{-1}[(\langle I^+\rangle-\langle S^+\rangle)$$

$$+(i/\langle\gamma\rangle\tau_c\,(\langle S_L\rangle\langle I^+\rangle-\langle I_L\rangle\langle S^+\rangle)]\,, \tag{6}$$

where $\langle I^+\rangle$ ($\langle S^+\rangle$) is the expectation value of the transverse nuclear (electronic) polarization, defined in the usual way. The imaginary term of Eq. (6) is the shift of the nuclear Zeeman energy levels due to the spin-exchange interaction. Equations analogous to Eqs. (2) and (6) can be written for the spin polarization of the alkali valence electron.

Since the time constants associated with the alkali electronic spin are about three orders of magnitude shorter than those associated with the noble-gas nuclear spin, we can treat the alkali spin as if it were in steady state, when considering the noble-gas nuclear-spin dynamics. Then, in the presence of other relaxation mechanisms, the rate of change of the longitudinal noble-gas nuclear spin becomes

$$\langle\dot{I}_L\rangle=-T_{ex}^{-1}(\langle I_L\rangle-\langle S_L^0\rangle)-T_1^{-1}\langle I_L\rangle\,, \tag{7}$$

where $\langle S_L^0\rangle$ denotes the steady-state value of the alkali polarization. The steady-state noble-gas nuclear polarization is then found to be

$$\langle I_L^0\rangle=T_p/T_{ex}\langle S_L^0\rangle\,, \tag{8}$$

where $T_p^{-1}=T_{ex}^{-1}+T_1^{-1}$, and T_1^{-1} is the sum of all other rates contributing to the longitudinal relaxation of the noble-gas nuclear spin.

Measurement of the transverse nuclear-spin polarization is accomplished by causing the polarized ensembles of both the noble gas and alkali atoms to precess in a plane containing the light beam. If the time average of the alkali transverse polarization is zero in a Larmor period of the noble-gas nucleus, then by Eq. (6), the time dependence of the transverse noble-gas spin polarization can be shown to have the following form:

$$\langle I^+(t)\rangle=\langle I_L^0\rangle\exp(-t/T_2)\sin(\Omega T+\psi)\,, \tag{9}$$

where T_2 is the total transverse decay time, Ω is the precessional frequency of the nuclear ensemble, and ψ is the initial phase of the precessing ensemble.

III. EXPERIMENTAL

The experimental apparatus

The experimental apparatus is shown schematically in Fig. 1. The apparatus consists of the experimental cell, which is a 15-ml Pyrex sphere. Cells are prefilled on a separate vacuum system with an excess of ^{87}Rb metal, 0.5 Torr ^{129}Xe, and N_2 as a buffer gas.

The cell is centered in a resistance-heated oven provided with Pyrex windows at either end. The oven provides controlled temperatures to 80 °C (±0.1 °C) with a temperature uniformity across the cell of about 1 °C. The oven is contained in a cylindrical coil form, providing three mutually perpendicular Helmholtz coils arranged along the x, y, and z axes. In addition correction turns along the x axis allow for the correction of magnetic field gradients, and a pair of reverse Helmholtz coils along the y and z axes provide a source of nuclear relaxation (magnetic field gradient relaxation)[2] in order to be able to force the nuclear magnetization to zero. The oven assembly is within four cylindrically concentric magnetic shields with the innermost shield provided with endcaps with 3-inch access holes. The magnetic shields reduce the external magnetic fields to below 10 μG.

The light source of the optical pumping and detection is an alkali resonance lamp of the Bell, Bloom, Lynch type.[11] The light is passed through a D_1 filter and a circular polarizer and piped to the cell through a plastic light pipe. On the detection side, the light transmitted through the cell is piped through a plastic light pipe to a photodiode.

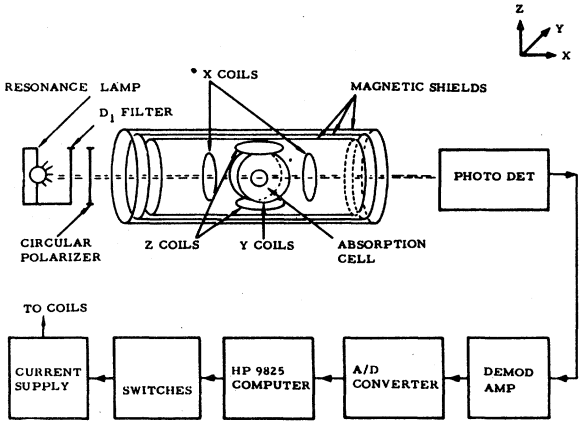

FIG. 1. Schematic representation of the experimental apparatus.

Polarization of the noble-gas nuclear-spin ensemble

The noble-gas nuclei are polarized through spin-exchange collisions with the optically oriented alkali vapor. The alkali vapor is polarized by the absorption of σ^+ D_1 light in a standard longitudinal pumping scheme; this configuration is shown in Fig. 2. The pumping takes place in the presence of a longitudinal magnetic field of approximately 2 mG. From Eqs. (7) and (8) one sees that the longitudinal noble-gas polarization obeys the following pumping law, given the initial condition $\langle I_L(t=0)\rangle$:

$$\langle I_L(t)\rangle = \langle I_L^0\rangle[1-\exp(-t/T_p)]\,. \tag{10}$$

The nuclear spins are "pumped" for a time sufficient to build up a significant polarization along the light beam direction. This time can range from 30 min. at cell temperatures below 40 °C to a few minutes at cell temperatures above 70 °C.

Detection of the transverse spin decay of the noble-gas nuclei

Measurement of the decay of the noble-gas nuclear-spin polarization is accomplished by switching the longitudinal pump field off and at the same time applying a precessional field along the y axis (~100 μG). The fields are switched in a time short enough to guarantee that the spin systems precess about the y axis. An ac field (8 kHz) is then applied along the z axis, to utilize the alkali vapor as a magnetometer, as discussed below. The equivalent field associated with the precessing nuclear moments is detected by the magnetometer, and thus the decay characteristics of the nuclear-spin systems are observed. The magnetic field arrangement for the detection mode is shown in Fig. 3.

The alkali magnetometer

The magnetometer mechanization of the alkali vapor, which we use to detect the noble-gas nuclear polarization, was first devised by Cohen-

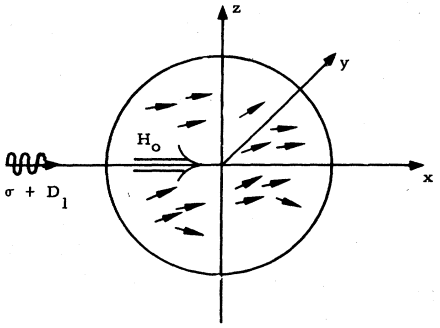

FIG. 2. Magnetic field arrangement for the longitudinal pumping of the alkali vapor.

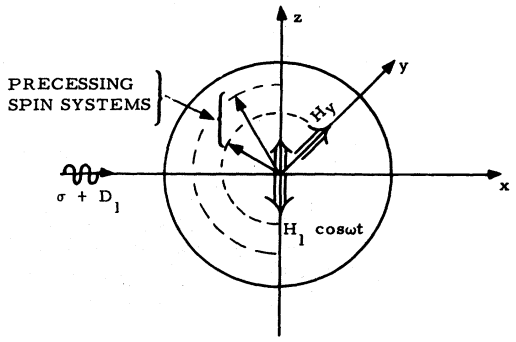

FIG. 3. Magnetic field arrangement for the detection of the noble-gas nuclear spins.

Tannoudji *et al.*[12] and first used to detect[13] the nuclear polarization of ^{3}He. We quote from their results as they apply to our experiment.

Consider an alkali vapor cell, as shown in Fig. 4, illuminated by σ^+ D_1 light along the x axis in the presence of a static magnetic field H_0 and an ac magnetic field $H_1\cos(\omega t)$, both applied along the z axis. The intensity of the transmitted light through the cell in this configuration has been shown to be sensitive to the x component of the alkali magnetization.[14] From Ref. 10, we write the transverse alkali polarization as

$$\frac{M^+}{M_0'} = A_0 + \sum_{p=1}^{\infty}\left[A_p\exp(ip\omega t) + A_{-p}\exp(-ip\omega t)\right], \tag{11}$$

where M_0' is defined by the steady-state alkali magnetization in the presence of relaxation and

$$A_0 = \sum_{n=-\infty}^{\infty}\frac{J_n^2(\omega_1/\omega)}{1+i(\omega_0+n\omega)\tau} \tag{12a}$$

and

$$A_p = \sum_{n=-\infty}^{\infty}\frac{J_n(\omega_1/\omega)J_{n\mp p}(\omega_1/\omega)}{1+i(\omega_0+n\omega)\tau}\,, \tag{12b}$$

where $\omega_0 = H_0\gamma_A$, $\omega_1 = H_1\gamma_A$ with γ_A the gyromagnet-

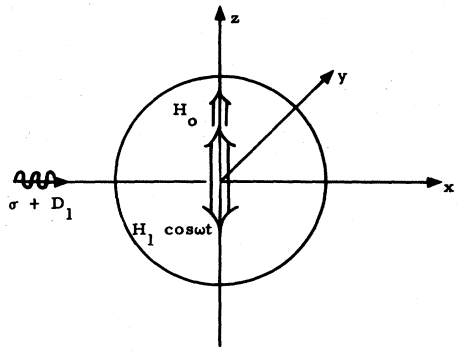

FIG. 4. Magnetic field arrangement for the magnetometer mechanization of the alkali vapor.

ic ratio of the alkali valence electron, τ is the spin relaxation time of the alkali vapor, and $J_n(\omega_1/\omega)$ is a Bessel function of order n when $n \geq 0$. For $n<0$, one has

$$J_n(\omega_1/\omega) = (-1)^n J_{-n}(\omega_1/\omega) . \quad (13)$$

Since $M_x = \mathrm{Re}M^+$ we can deduce the behavior of M_x and hence the optical signal from Eqs. (11), (12a), and (12b). One sees then that M_x is a periodic function in time with period $2\pi/\omega$, and the light transmitted through the cell is modulated at various harmonics p of $p\omega$ which depends on A_p and A_{-p} given in Eq. (12b). In addition one can see that the signal undergoes a resonance when the field is swept about the value for which $(\omega_0 + n\omega) = 0$. Thus at each modulation, p resonates from $\omega_0 = 0$, $\omega_0 = \pm\omega, \ldots$. The width of these resonances is independent of n and is $\Delta\omega_0 = 2/\tau$. The amplitude of the resonance of order n, detected at the harmonic p, is given by the Bessel function $J_n(\omega_1/\omega)J_{n\pm p}(\omega_1/\omega)$.

In our experiment we operate at the $n=0$ resonance and detect the $p=1$ modulation. For the case of a constant magnetic field along the z axis the signal is found to have the following proportionality:

$$S\alpha M_0' J_0\left(\frac{\omega_1}{\omega}\right) J_1\left(\frac{\omega_1}{\omega}\right) \frac{\omega_0}{1+(\omega_0\tau)^2} \sin(\omega t) \quad (14)$$

for $\omega_0 \ll 1$; the signal is seen to be proportional to the field along the z axis in first order.

In our experimental arrangement, because of the presence of the y-axis precessional field and because of the rotation of the nuclear field in the x, z plane, there are fields along all three axes. The expression for the signal in the $n=0$, $p=1$ mode for the case of a general magnetic field is given by[15]

$$S\alpha \frac{M_0'}{\Gamma} J_0\left(\frac{\omega_1}{\omega}\right) J_1\left(\frac{\omega_1}{\omega}\right) \frac{\Gamma\bar{\omega}_z + \bar{\omega}_x\bar{\omega}_y}{\Gamma^2 + \bar{\omega}_x^2 + \bar{\omega}_y^2 + \bar{\omega}_z^2} \sin(\omega t) , \quad (15)$$

where $\Gamma = 1/\tau$, $\bar{\omega}_z = \omega_z$, and $\bar{\omega}_{y,x} = J_0(\omega_1/\omega)\gamma_A H_{y,x}$ with

$$\omega_z = \gamma_A H_e^{\mathrm{NG}} \cos(\Omega t) , \quad (16a)$$

$$\omega_x = \gamma_A H_e^{\mathrm{NG}} \sin(\Omega t) , \quad (16b)$$

where H_e^{NG} is the magnitude of the equivalent magnetic field due to the noble-gas nuclei, as seen by the alkali atoms. Since $\Omega \ll \omega$, we take the nuclear field as approximately dc and substitute the expressions given in Eqs. (16a) and (16b) directly into Eq. (15), using the condition $\Gamma \gg \omega_x, \omega_z$. Then one finds

$$M_0' J_0\left(\frac{\omega_1}{\omega}\right) J_1\left(\frac{\omega_1}{\omega}\right) \gamma_A H_e^{\mathrm{NG}} \times \frac{[\Gamma^2 + J_0^4(\omega_1/\omega)\gamma_A^2 H_y^2]^{1/2}}{\Gamma^2 + J_0^2(\omega_1/\omega)\gamma_A^2 H_y^2} \cos(\Omega t + \psi)\sin(\omega t) . \quad (17)$$

The signal then is seen to be proportional to the magnitude of the nuclear field, doubly modulated at the frequency ω and the nuclear precession frequency Ω.

The experimental procedure

A measurement of the noble-gas transverse decay rate is made in the following manner. An experimental cell is situated in the apparatus. The fields present at the cell are balanced to zero with the Helmholtz coils on each axis by employing the results of the signal expression in Eq. (15). At first all fields are close to zero with no compensation due to the magnetic shielding. Next a low-frequency (10-Hz) external sinusoidal field is applied along either the x or y axes; the induced signal can then be minimized by forcing the field along the y or x directions, respectively, to zero by applying a compensating field with the appropriate Helmholtz coil. The z axis can be compensated by applying a dc field that forces the dc component of the induced signal to zero. The signal sensitivity is then maximized by applying the external field along the z axis and then adjusting the ac amplitude ω_1 to maximize the Bessel function product $J_0(\omega_1/\omega)J_1(\omega_1/\omega)$. A longitudinal noble-gas polarization can now be attained by applying a dc field along the direction of the light beam.

In our experimental measurements the detection light is blocked, for the most part, during the decay of the nuclear spin. The cell is illuminated for about a noble-gas Larmor period at the beginning of the decay and again some time later. The noble-gas relaxation time T_2 is deduced from Eq. (9) knowing the signal strengths at the times when the cell is illuminated and the time the spin decaying in the "dark." This procedure ensures that the transverse alkali spin is zero and hence decoupled from the noble-gas spin decay.

IV. RESULTS

The total transverse decay rate $1/T_2$ defined in Eq. (9), is assumed to be of the form

$$T_2^{-1} = T_{\mathrm{ex}}^{-1} + (T_2')^{-1}$$

$$= N_{\mathrm{Rb}}\sigma_{\mathrm{ex}}\bar{V} + (T_2')^{-1} , \quad (18)$$

where to first order, the variation of T_2 to temperature is due to spin exchange. Observing from Eqs. (5) that the spin-exchange cross section is inversely proportional to the relative velocity squared, we plot in Fig. 5 typical relaxation rate data versus the term $N_{\mathrm{Rb}}/\bar{V}$. We have taken the Rb number density to be given by the saturated formula[16]

$$\log_{10} N_{\mathrm{Rb}} = -4560/T + 30.98 - 2.45\log_{10} T , \quad (19)$$

where T is the cell temperature in kelvin. We perform a linear least-squares fit to the data such as that represented in Fig. 5. The estimate of the slope corresponds to the temperature-independent exchange term $\sigma\bar{V}^2$, and the intercept represents the sum of all other relaxation rates $1/T_2'$, which in the case of ^{129}Xe is mostly due to magnetic field gradient relaxation. Finally, in Fig. 6, we plot the measured spin-exchange cross section versus N_2 buffer density in the cell.

The role of molecular formation in the spin-exchange process

We believe that the results displayed in Fig. 6 are an indication of a role of the Rb-Xe diatomic molecule in the spin-exchange process. The solid line curve in Fig. 6 represents a least-squares fit of the data to a simplistic molecular model of the exchange process.

We take the exchange rate between the Rb electronic spin and the Xe nuclear spin to have contributions from bound-molecular-type collisions and binary-type collisions, which are independent, and hence we can write the total exchange rate at

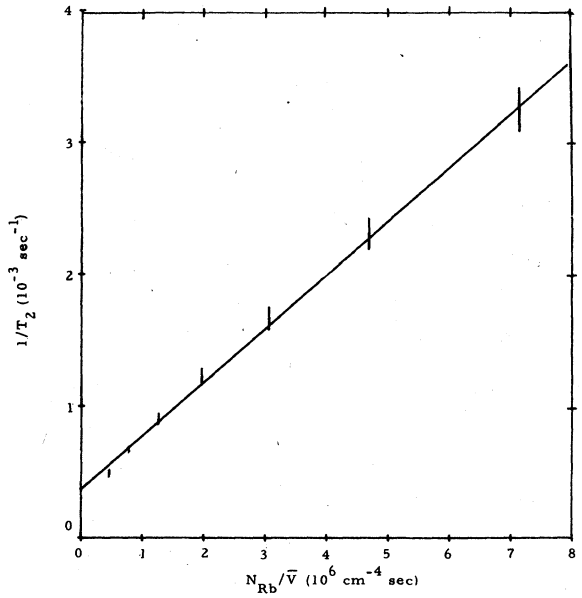

FIG. 5. Typical plot of the Xe relaxation rate versus $N_{Rb}\bar{V}$. The solid line represents a linear least-squares fit of the experimental data, where the slope of the line represents the spin-exchange cross-section term, and the intercept is the sum of all other relaxation rates. The error bars on the data points are a standard deviation of repeated trials. These data were taken from a cell containing ^{87}Rb, 0.5 Torr ^{129}Xe and 74.5 Torr N_2. The least-squares fit yielded a temperature independent rate of $(3.67 \pm 0.3) \times 10^{-4}$ sec^{-1} and $\sigma_{ex}\bar{V}^2 = (4.07 \pm 0.35) \times 10^{-10}$ cm^{4}sec^{-2}.

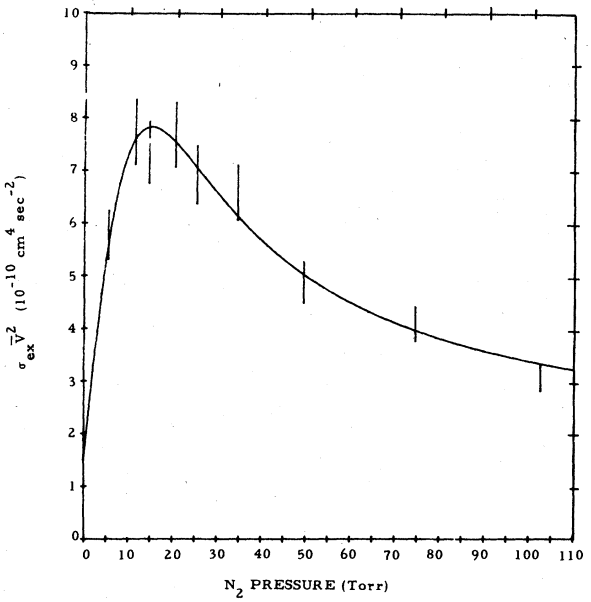

FIG. 6. Plot of the spin-exchange cross-section term versus the N_2 pressure. The solid line is least-squares fit of the data to our molecular spin-exchange model. The error bars on the data points represent a standard deviation for repeated trials.

$$T_{ex}^{-1} = T_{ex}^{-1}(\text{molecule}) + T_{ex}^{-1}(\text{binary}), \tag{20}$$

where both contributions can be written in terms of a spin-exchange cross section as in Eq. (4). We neglect the effects of quasi-bound molecules following the results of a previous study of the Rb-Xe molecule.[17] For bound molecules, which are formed in three-body collisions, we take the third body to be an N_2 molecule, which is always by far in greatest abundance. In this case then, we have that the molecular formation rate is proportional to the density of N_2. Taking the correlation time of the interaction to be the duration of the collision, then τ_c is inversely proportional to the density of N_2, since the Rb-Xe molecule exists only until it experiences a collision. Again, because of the relative number densities in this work, we take the breakup body always to be an N_2 molecule. The short binary collisions between the Rb and Xe atoms are independent of the N_2 density. As a function of N_2 density we can rewrite Eq. (20) as

$$T_{ex}^{-1} = (a\rho)\tfrac{1}{2}\frac{(b/\rho^2)}{1+(b/\rho^2)} + c\,. \tag{21}$$

Rearranging the terms we find

$$T_{ex}^{-1} = \tfrac{1}{2}\frac{ab\rho}{b+\rho^2} + c\,, \tag{22}$$

where ρ is the density of N_2, the factor a corre-

sponds to the molecular formation rate, b represents the average interaction strength correlation time product, and c is simply the binary exchange rate.

Evaluation of the parameters

A least-squares fit of our data to the functional form of Eq. (22) yielded the following information:

(1) The three-body collision rate of Rb, Xe, and N_2 per Xe atom was found to be

$$T_f^{-1} = (4.5 \pm 0.5) \times 10^{-4} \text{ sec}^{-1}/\text{Torr } N_2 \quad (23)$$

when evaluated at 273 K. Bouchiat *et al.*[18] evaluated the formation rate of Rb-Xe molecules in the presence of Xe only. Normalizing our formation rate per Torr Xe and converting to a formation rate per Rb atom, we find that our value differs from the one reported by Bouchiat by about 12%. The significance of this comparison lies only in the order-of-magnitude agreement, since the work of Bouchiat *et al.* was concerned with a different three-body collision.

(2) The average strength of the interaction multiplied by the duration of the collision per Torr N_2 was found to be

$$\langle\gamma\rangle\tau_c \sim 15 . \quad (24)$$

If we assume that the lifetime of the molecule is limited by N_2 collision, we can use standard gas kinetic arguments to estimate

$$\tau_c = 0.5 \times 10^{-7} \text{ sec/Torr } N_2 . \quad (25)$$

Substituting this value into Eq. (24), we find the average interaction strength:

$$\langle\gamma\rangle \sim 3 \times 10^8 \text{ sec}^{-1} . \quad (26)$$

This value is only of order-of-magnitude agreement with that estimated previously for the binary collisions,[7,8] but that seems to be reasonable agreement considering the approximations used in the theory.

(3) The binary spin-exchange term was found to be

$$\sigma_{ex}\bar{V} = (1.5 \pm 0.2) \times 10^{-10} \text{ cm}^4 \text{ sec}^{-2} . \quad (27)$$

A previous measurement of the exchange cross section for ^{87}Rb-^{129}Xe was made by Grover[6] in cells buffered with 500 Torr He^4. Extrapolating our values for N_2 out of 500 Torr, we find a difference of about 30% between our value and Grover's. The difference may lie in either different molecular kinematics for He-buffered cells or in the fact that Grover's relaxation measurements were not done in the "dark," which would possibly have resulted in a distortion of the Xe relaxation signal.

Evaluating the spin-exchange cross section at 65 °C, we find $\sigma_{ex} = 1.1 \times 10^{-19}$ cm^2. This value is about four times larger than what had been theoretically estimated using the Herman-Skillman wavefunction tabulations.[8] We think that this is reasonable agreement considering the uncertainty in the parameters that enter into the calculations. For instance the entire factor of 4 could result from only a 20% error in the Rb wave function because this parameter enters twice, each time raised to the fourth power.

V. SUMMARY

The measurement of the ^{87}Rb-^{129}Xe spin-exchange cross section has indicated a significant role of the Rb-Xe van der Waals molecule in the spin-exchange process. Our estimate of the molecular formation rate for the Rb-Xe molecule is in reasonable agreement with the previously measured formation rate,[18] which we take to be supportive of our model of molecular-enhanced spin exchange. Although our estimate of the Rb-Xe spin-exchange cross section is much larger than theoretical estimates, we think that the overall agreement is generally good, and discrepancies are indicative of the uncertainties in the theory.

Since there has been recent evidence for the existance of alkali-atom-noble-gas-atom van der Waals molecules with light noble gases,[19] one might expect a similar molecular-enhanced spin-exchange cross section for ^{3}He and ^{21}Ne, which may be of interest in the consideration of polarized nuclear targets.

The attainable nuclear polarization is seen from Eq. (8) to depend on the T_1 relaxation of the nuclear ensemble and the saturated value of the alkali polarization. In our study of ^{129}Xe, the dominant source of T_1 relaxation was due to magnetic field-inhomogeneities. Achieving nuclear polarizations better than 90% of the alkali polarization in our present apparatus would imply cell temperatures of greater than only 60 °C, for a sample buffered with between 15 and 25 Torr N_2. We note that the field inhomogeneities could have been further reduced from what we tolerated in our experiment through the use of higher-order corrections on the magnetic field. This would have in effect lowered the already moderate cell temperature at which one could attain relatively high nuclear polarizations. Alkali ground-state polarizations approaching 100%, through the use of laser pumping, have recently been reported[20] in samples of Na with densities of 10^{12} cm^{-3}. This alkali density is an order of magnitude larger than the Rb densities in our experiment. It is then quite feasible to expect nuclear polarizations approaching 100% in controlled environments through exchange with a laser-pumped alkali vapor ensemble.

ACKNOWLEDGMENTS

We would like to acknowledge the contributions of Dr. E. Kanegsberg in the area of observing alkali-atom-noble-gas-nucleus spin exchange using the magnetometer technique and for his helpful comments in the preparation of this paper. We are also thankful for the talents of R. L. Meyer and H. E. Williams for their design and construction of the apparatus used in this work. This reasearch was partially supported under an Air Force Office of Scientific Research Contract No. F49620-77-C-0047.

---

[1]M. A. Bouchiat, T. R. Carver, and C. M. Varnum, Phys. Rev. Lett. 5, 373 (1960).
[2]R. L. Gamblin and T. R. Carver, Phys. Rev. 138, A946 (1965).
[3]W. A. Fitzsimmons, L. L. Tankersley, and G. K. Walters, Phys. Rev. 179, 156 (1969).
[4]H. Sobell, Z. Naturforsch. 24, 2023 (1969); Phys. Lett. 41A, 373 (1972); Z. Phys. 265, 487 (1973).
[5]R. M. Herman, Phys. Rev. 137, A1062 (1965).
[6]B. C. Grover, Phys. Rev. Lett. 40, 391 (1978).
[7]F. G. Major, Litton Subcontract Report No. WC376807 (unpublished).
[8]C. H. Volk, B. C. Grover, and E. Kanegsberg, AFOSR, Annual Technical Report, 1978 (unpublished).
[9]H. G. Dehmelt, Phys. Rev. 109, 381 (1958).
[10]L. C. Balling, R. J. Hanson, and F. M. Pipkin, Phys. Rev. 133, A607 (1964).
[11]W. E. Bell, A. L. Bloom, and J. Lynch, Rev. Sci. Instrum. 32, 688 (1961).
[12]C. Cohen-Tannoudji, J. Depont-Roc, S. Haroch, and F. Laloe, Rev. Phys. Appl. 5, 102 (1970).
[13]C. Cohen-Tannoudji, J. Dupond-Roc, S. Haroch, and F. Laloe Phys. Rev. Lett. 22, 758 (1969).
[14]M. A. Bouchiat, J. Phys. (Paris) 26, 415 (1965).
[15]J. Depont-Roc, Rev. Phys. Appl. 5, 853 (1970).
[16]C. J. Smithells, *Metals Reference Book* (Butterworths, London, 1962), Vol. 2, p. 655.
[17]C. C. Bouchiat, M. A. Bouchiat, L. C. L. Pottier, Phys. Rev. 181, 3144 (1969).
[18]M. A. Bouchiat, J. Brossel, and L. C. Pottier, J. Chem. Phys. 56, 3703 (1972).
[19]F. A. Franz and C. H. Volk, Phys. Rev. Lett. 35, 1704 (1975); Phys. Rev. A 14, 1711 (1976); 18, 599 (1978).
[20]A. C. Tam and W. Happer, Appl. Phys. Lett. 30, 580 (1977).